Dinuclear Copper(II) Complexes with Carboxylate-Rich Coordination Environments. Models for Substituted Copper(II) Aminopeptidases

Richard C. Holz,*,† Julie M. Brink,† Feben T. Gobena,† and Charles J. O'Connor‡

Department of Chemistry and Biochemistry, Utah State University, Logan, Utah 84322-0300, and Department of Chemistry, University of New Orleans, New Orleans, Louisiana 70122

Received October 15, 1993[⊗]

The dinucleating ligand *N,N'*-(2-hydroxy-5-methyl-1,3-xylylene)bis(*N*-carboxymethylglycine) (CH_3HXTA) has been used to synthesize the dinuclear Cu(II) diaqua complex $[Cu_2(CH_3HXTA)(H_2O)_2]H{\cdot}4H_2O$ (**1**): monoclinic space group $P2_1/n$ (a = 15.092(3) Å, b = 10.842(3) Å, c = 15.219(4) Å, and β = 104.70(2)°). The structure shows two distinct square pyramidal Cu(II) centers with each Cu(II) ion bound to two carboxylate oxygen atoms, one amine nitrogen atom, the phenolate oxygen atom, and one water oxygen atom. The Cu- -Cu separation is 3.726 Å and Cu1−O1−Cu2 angle is 127.9°. The phenyl ring of the CH_3HXTA ligand is twisted relative to the Cu1−O1−Cu2 plane and the resulting dihedral angle is 46.7°. The electronic absorption and EPR spectra of **1** in aqueous solution at pH 3 suggest a shift toward trigonal bipyramidal Cu(II) coordination in solution. Variable temperature magnetic susceptibility data for **1** indicates that it behaves as a simple Curie−Weiss paramagnet and hence the Cu(II) ions show little coupling ($J \sim 0$). Titration of **1** with sodium hydroxide is accompanied by a reversible shift in the phenoxide-to-copper LMCT band at 420 nm and a concomitant decrease in the molar absorptivity. These data suggest that **1**, is converted to a second dicopper(II) complex (**2**) with an apparent pK_a of 8. The structure of **2**, derived from electronic absorption, EPR, NMR, and Evans susceptibility measurements, indicate it is the (μ-phenoxo)(μ-hydroxo)dicopper(II) complex $[Cu_2(CH_3HXTA)(\mu\text{-}OH)]^{2-}$.

Introduction

Many di- and trinuclear metalloprotein active sites have recently been recognized to have carboxylate-rich coordination environments.[1−3] Enzymes in this group include the crystallographically characterized B2 subunit of ribonucleotide reductase,[4] methane monooxygenase,[5] phospholipase C,[6] alkaline phosphatase,[7] P1 nuclease,[8] and the aminopeptidases.[9−12] Additional enzymes, such as the purple acid phosphatases[13,14] and rubrytherin[15] may also be included in this group based on spectroscopic data. These dinuclear enzymes utilize a wide variety of metal ions that include magnesium, calcium, manganese, iron, cobalt, and zinc. They are involved in a wide range of chemical reactions that include C-H activation, dioxygen activation, electron transfer, or hydrolytic chemistry. The structural aspects of these sites, such as coordination geometry and number of carboxylate residues, very likely dictate the level and type of activity.

Of particular interest are the crystallographically characterized aminopeptidases. Bovine lens leucine aminopeptidase (blLAP) contains a bis(μ-carboxylato)dizinc(II) core with terminal carboxylates at each metal site along with a peptide backbone carbonyl and a lysine amine nitrogen.[10,11] Methionine aminopeptidase (MAP) from *E. coli* contains a bis(μ-carboxylato)-dicobalt(II) core with terminal carboxylates at each metal site along with a single histidine residue.[9] In both MAP and blLAP the metal−metal distance is 2.9 Å. The third aminopeptidase from *Vibrio proteolytica* (AP) possesses a (μ-aqua)(μ-carboxylato)dizinc(II) core with one terminal carboxylate and one histidine residue at each metal ion.[12] Both Zn(II) ions in AP appear to be in distorted trigonal bipyramidal coordination environments with a Zn-Zn distance of 3.5 Å. The structural motifs observed for these three aminopeptidases are unusual for zinc proteases since most mononuclear hydrolytic zinc sites, such as those found in carboxypeptidases and endopeptidases, are histidine rich.[16]

AP and blLAP can be fully or partially activated by a large variety of metal ions that include Mg(II), Mn(II), Fe(II), Co(II), Ni(II), and Cu(II).[17−19] For AP, substitution of the two g-atoms of Zn(II) with Co(II), Cu(II), or Ni(II) provides different magnitudes of activity that are dependent on the sequence and order of addition of the metal ions.[17,18,20] It was reported that Cu(II), Co(II), or Ni(II) substituted AP is hyperactive by 6.5,

† Utah State University.
‡ University of New Orleans.
⊗ Abstract published in *Advance ACS Abstracts,* November 1, 1994.

(1) Fenton, D. E.; Okawa, H. *J. Chem. Soc. Dalton Trans.* **1993**, 1349−1357.
(2) Feig, A. L.; Lippard, S. J. *Chem. Rev.* **1994**, *94*, 759−805.
(3) Vallee, B. L.; Auld, D. S. *Biochemistry* **1993**, 6493−6500.
(4) Norland, P.; Sjöberg, B.-M.; Eklund, H. *Nature* **1990**, *345*, 593−598.
(5) Rosenzweig, A. C.; Federick, C. A.; Lippard, S. J.; Nordlund, P. *Nature* **1993**, *366*, 537−543.
(6) Hough, E.; Hansen, L. K.; Birknes, B.; Jynge, K.; Hansen, S.; Horvik, A.; Little, C.; Dodson, E.; Derewenda, Z. *Nature* **1989**, *338*, 357−360.
(7) Kim, E. E.; Wyckoff, H. W. *J. Mol. Biol.* **1991**, *218*, 449−464.
(8) Lahm, A.; Volbeda, A.; Suck, D. *J. Mol. Biol.* **1990**, *215*, 207−210.
(9) Roderick, S. L.; Matthews, B. W. *Biochemistry* **1993**, *32*, 3907−3912.
(10) Burley, S. K.; David, P. R.; Taylor, A.; Lipscomb, W. N. *Proc. Natl. Acad. Sci. USA* **1990**, *87*, 6878−6882.
(11) Burley, S. K.; David, P. R.; Sweet, R. M.; Taylor, A.; Lipscomb, W. N. *J. Mol. Biol.* **1992**, *224*, 113−140.
(12) Chevrier, B.; Schalk, C.; D'Orchymont, H.; Rondeau, J.-M.; Moras, D.; Tarnus, C. *Structure* **1994**, *2*, 283−291.
(13) Holz, R. C.; Que, L. J.; L.-J., M. *J. Am. Chem. Soc.* **1992**, *114*, 4434−4436.
(14) True, A. E.; Scarrow, R. C.; Randall, C. R.; Holz, R. C.; Que, L. J. *J. Am. Chem. Soc.* **1993**, *115*, 4246−4255.
(15) Ravi, N.; Prickril, B. C.; Kurtz, D. M.; Huynh, B.-H. *Biochemistry* **1993**, *32*, 8487−8491.
(16) Vallee, B. L.; Auld, D. S. *Biochemistry* **1990**, *29*, 5647−5659.
(17) Prescott, J. M.; Wagner, F. W.; Holmquist, B.; Vallee, B. L. *Biochem. Biophys. Res. Commun.* **1983**, *114*, 646−652.
(18) Prescott, J. M.; Wagner, F. W.; Holmquist, B.; Vallee, B. L. *Biochemistry* **1985**, *24*, 5350−5356.
(19) Allen, M. P.; Yamada, A. H.; Carpenter, F. H. *Biochemistry* **1983**, *22*, 3778−3783.
(20) Bayliss, M. E.; Prescott, J. M. *Biochemistry* **1986**, *25*, 8113−8117.

0020-1669/94/1333-6086$04.50/0

7.7, and 25 times, respectively. The addition of 1 mol of Cu(II), Co(II), or Ni(II) to the apoenzyme followed by the addition of Zn(II) enhances the enzymatic activity to an even greater extent. For Ni(II) and Cu(II), nearly a 90- and 100-fold increase in activity is observed, respectively. To our knowledge, this is the only Zn(II) enzyme that can be hyperactivated by Cu(II). Since no spectral data of any kind has been reported for the Ni(II) or Cu(II) substituted AP enzymes, structural modifications leading to the hyperactivity of these metal substituted enzymes are unknown.

The synthesis and characterization of dinuclear Cu(II) complexes have received a great deal of attention due to their presence in hemocyanin, tyrosinase, laccase, and ascorbate oxidase.[21-25] Binucleating ligands that contain a phenolate donor group have been used extensively to model these dinuclear Cu(II) metalloprotein active sites. The majority of these complexes contain pyridine, imidazole, benzimidazole, or pyrazole groups as terminal ligands. These complexes serve as excellent models for dicopper(II) centers found in enzymes with histidine rich coordination environments; however, a systematic investigation of dicopper(II) centers in carboxylate rich coordination environments has yet to be reported. In an effort to model the carboxylate rich coordination environment of the hyperactive dicopper(II) center of AP, we have synthesized the dinuclear Cu(II) complex $[Cu_2(CH_3HXTA)(H_2O)_2]H{\cdot}4H_2O$ (**1**) (where CH_3HXTA = *N,N'*-(2-hydroxy-5-methyl-1,3-xylylene)bis(*N*-carboxymethylglycine). This complex has been characterized by X-ray crystallography, electronic absorption, NMR, and EPR spectroscopies as well as magnetic susceptibility. The conversion of **1** to a second complex **2** is observed upon the addition of sodium hydroxide. Complex **2** has been spectroscopically characterized as the (μ-phenoxo)(μ-hydroxo)dicopper(II) CH_3HXTA complex.

Experimental Methods

Synthetic Methods. All chemicals were purchased commercially and used as received. *N,N'*-(2-hydroxy-5-methyl-1,3-xylylene)bis(*N*-carboxymethylglycine) (CH_3HXTA) was synthesized from *p*-cresol, iminodiacetic acid, and formaldehyde according to the method of Schwarzebach *et al.*[26] with minor revisions as reported by Murch *et al.*[27] Substituted X-HXTA derivatives where X = Cl, CN, and CH_3O were all prepared in a similar manner to CH_3HXTA except that the appropriate para-substituted phenol was used in place of *p*-cresol. The identities of each ligand were confirmed by ^1H NMR spectroscopy. ^1H NMR (D_2O, δ 4.70): CH_3HXTA δ 2.31 (s, 3 H), 3.26 (s, 8 H), 3.78 (s, 4 H), 7.06 (s, 2 H); ClHXTA δ 3.07 (s, 8 H), 3.60 (s, 4 H), 7.03 (s, 2 H); CNHXTA δ 3.33 (s, 8 H), 3.90 (s, 4 H), 7.39 (s, 2 H); CH_3OHXTA δ 3.07 (s, 8 H), 3.61 (s, 3 H), 3.65 (s, 4 H), 6.67 (s, 2 H). *Caution*: It has previously been reported that CH_3HXTA can cause allergic reactions.[27]

The general procedure for the synthesis of dinuclear Cu(II) complexes of CH_3HXTA are as follows. CH_3HXTA (0.60 g; 1.2 mmol) was dissolved in 20 mL of H_2O. To this solution 0.96 g (2.4 mmol) of Cu(II) perchlorate hexahydrate dissolved in 2 mL of H_2O was added. The solution immediately turned dark green (pH ~3.0). Upon standing overnight, green rectangular plates of **1** were deposited. The analytical purity of **1** was checked by elemental analysis (Atlantic Microlab, Inc.). Calcd for $[Cu_2(CH_3HXTA)(H_2O)_2]H{\cdot}4H_2O$ (**1**) ($C_{17}H_{29}Cu_2N_2O_{15}$): C, 32.49; H, 4.65; N, 4.46. Found: C, 32.63; H, 4.52; N, 4.52. Complex **2** was prepared by dissolving 0.1 g of **1** in 1 mL of H_2O and adjusting the pH to 10.

Table 1. Summary of Crystallographic Data for $[Cu_2(CH_3HXTA)(H_2O)_2]H{\cdot}4H_2O$

empirical formula	$C_{17}H_{29}N_2O_{15}Cu_2$
fw	628.09
cryst system	monoclinic
space group	$P2_1/n$ (No. 14)
a (Å)	15.092(3)
b (Å)	10.842(3)
c (Å)	15.219(4)
α (deg)	90
β (deg)	104.70(2)
γ (deg)	90
V (Å^3)	2409(1)
Z	4
ϱ_{calc} (g cm^{-3})	1.733
μ (mm^{-1})	1.843
radiation	Mo Kα (λ = 0.710 73 Å)
temp (°C)	−100
residuals:[a] R; R_w	0.041; 0.058

[a] $R = \sum||F_o| - |F_c||/\sum|F_o|$; $R_w = [(\sum w(|F_o| - |F_c|)^2/\sum wF_o^2)]^{1/2}$; $w = 1/\sigma^2(|F_o|)$.

Crystallographic Studies. Green rectangular crystals of **1**, suitable for X-ray diffraction studies, were grown by slow evaporation of an aqueous solution of **1** (pH ~3). A suitable crystal was selected and mounted in a 0.3 mm diameter X-ray capillary and centered optically on a Seimens P4 diffractometer equipped with an LT-2a low-temperature device that maintained the crystal at −100 °C throughout data collection. Autocentering of 25 reflections indicated a monoclinic cell. Systematic absences in the data set led to the unambiguous selection of the space group $P2_1/n$ (No. 14). Two standard reflections were measured every 50 reflections and remained constant (±1%) throughout the data collection. The copper atoms were located by Patterson methods, and the remaining non-hydrogen atoms were located by subsequent difference maps and refined anisotropically. Hydrogen atoms were generated in idealized positions with fixed thermal parameters (0.08). A summary of the crystallographic data collection for **1** is presented in Table 1, and the atomic coordinates and equivalent isotropic displacement coefficients are given in Table 2. The complete listing of the crystal data is provided in the supplementary material.

Physical Methods. Electronic absorption spectra were recorded on a Shimadzu UV-3101PC spectrophotometer. EPR spectra were measured at the X-band frequency with a Varian E-109 spectrometer equipped with an LN_2 coldfinger cryoscopic probe. ^1H NMR spectra were recorded in D_2O on either a Varian XL-300 or a Bruker ARX-400 spectrometer. Chemical shifts (in ppm) were referenced to the residual H_2O peak at 4.7 ppm. Elemental analyses were performed by Atlantic Microlabs, Inc. (Norcross, GA).

Magnetic susceptibility data were recorded over the temperature range 10 to 300 K at a measuring field of 2.0 kOe with an SHE Corp. VTS-50 superconducting SQUID susceptometer interfaced to an IBM 9000 computer system. Calibration and operating procedures have been reported elsewhere.[28]

Results and Discussion

Structural Studies. X-ray diffraction studies were carried out on $[Cu_2(CH_3HXTA)(H_2O)_2]H{\cdot}4H_2O$ (**1**). Compound **1** crystallizes in the space group $P2_1/n$. Four $[Cu_2(CH_3HXTA)(H_2O)_2]^-$ complexes are found in the unit cell along with four water molecules that form an intricate hydrogen bonding network. Hydrogen bonds are formed between the lattice water molecules and the carboxylate carbonyl oxygen atoms as well as the coordinated water molecules. The bound carboxylate oxygen O2 forms a hydrogen bond with a lattice water molecule resulting in the longest Cu−O carboxylate bond distance (1.985(4) Å).

(21) Kitajima, N.; Moro-oka, Y. *Chem. Rev.* **1994**, *94*, 737−757.
(22) Solomon, E. I.; Tuczek, F.; Root, D. E.; Brown, C. A. *Chem. Rev.* **1994**, *94*, 827−856.
(23) Sorrell, T. N. *Tetrahedron* **1989**, *45*, 3−68.
(24) Karlin, K. D.; Tyeklar, Z. *Bioinorganic Chemistry of Copper*; Chapman & Hill: New York, 1993.
(25) Karlin, K. D. *Science* **1993**, *262*, 1499.
(26) Schwarzenbach, G.; Anderegg, G.; Sallmann, R. *Helv. Chim. Acta* **1952**, *35*, 1785−1792.
(27) Murch, B. P.; Bradley, F. C.; Boyle, P. D.; Papafthymiou, V.; Que, L., Jr. *J. Am. Chem. Soc.* **1987**, *109*, 7993−8003.
(28) O'Connor, C. J. *Prog. Inorg. Chem.* **1982**, *29*, 203−283.

Table 2. Atomic Coordinates ($\times 10^4$) and Equivalent Isotropic Displacement Coefficients ($Å^2 \times 10^3$) for $[Cu_2(CH_3HXTA)(H_2O)_2]H{\cdot}4H_2O$

atom	x	y	z	U_{eq}[a]
Cu1	6326(1)	2765(1)	3058(1)	13(1)
Cu2	4622(1)	582(1)	1677(1)	13(1)
N1	6255(3)	2790(4)	4349(3)	11(1)
N2	4927(3)	−1258(4)	1692(3)	11(1)
O1	5537(2)	993(3)	2743(2)	16(1)
O2	5184(2)	3752(3)	2856(2)	18(1)
O3	4498(3)	5044(4)	3613(3)	31(1)
O4	7525(2)	1977(3)	3545(2)	16(1)
O5	8576(2)	1657(3)	4841(2)	18(1)
O6	3867(2)	210(3)	469(2)	17(1)
O7	3826(3)	−1027(4)	−705(2)	28(1)
O8	3628(3)	−144(3)	2476(3)	23(1)
O9	3093(3)	−1916(4)	2839(3)	27(1)
O10	6475(3)	3004(3)	1828(2)	18(1)
O11	4198(3)	2306(3)	1519(2)	22(1)
O12	7070(3)	5043(4)	3288(3)	32(1)
O13	3063(3)	5821(4)	2440(3)	25(1)
O14	3880(3)	5466(4)	921(3)	32(1)
O15	5803(3)	5248(4)	1413(3)	33(2)
C1	5825(3)	139(5)	3414(3)	14(2)
C2	5945(3)	501(5)	4321(3)	15(2)
C3	6268(3)	−376(5)	4999(3)	19(2)
C4	6472(3)	−1578(5)	4812(3)	18(2)
C5	6339(3)	−1918(5)	3898(3)	19(2)
C6	6027(3)	−1068(5)	3206(3)	15(2)
C7	5655(3)	1759(5)	4522(3)	16(2)
C8	7203(3)	2671(5)	4918(3)	16(2)
C9	7799(3)	2048(5)	4401(3)	14(2)
C10	5818(4)	3987(5)	4448(3)	18(2)
C11	5092(4)	4292(5)	3579(3)	18(2)
C12	5911(3)	−1441(5)	2230(3)	15(2)
C13	4287(3)	−2013(5)	2071(3)	16(2)
C14	3650(3)	−1271(5)	2488(3)	17(2)
C15	4825(3)	−1580(5)	719(3)	16(2)
C16	4105(3)	−769(5)	112(3)	14(2)
C41	6813(4)	−2512(5)	5551(4)	28(2)

[a] $U_{eq} = {}^1/_3\sum_i\sum_j U_{ij}a_i^*a_j^*a_ia_j$.

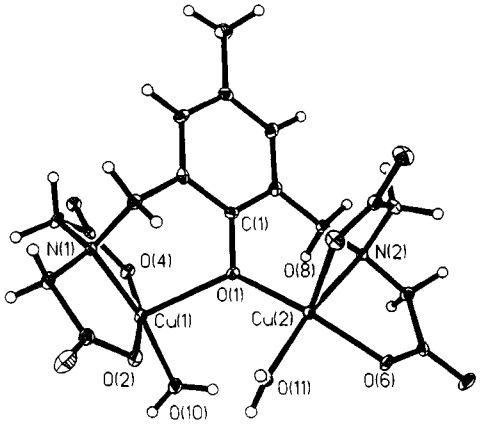

Figure 1. ORTEP drawing of the $[Cu_2(CH_3HXTA)(H_2O)_2]^-$ anion showing a partial numbering scheme. (Carbon and hydrogen atoms are not labeled for clarity.)

A thermal ellipsoid drawing of the cation of **1** with a partial labeling scheme is shown in Figure 1. Selected bond distances and angles are collected in Table 3. Each Cu(II) ion in **1** is bound to two carboxylate oxygen atoms, one amine nitrogen atom, the phenolate oxygen atom, and one water oxygen atom. Each Cu(II) ion exhibits a distorted square pyramidal geometry in nonidentical environments. The Cu1−O1 (μ-phenoxo oxygen) bond is 2.246(4) Å while the Cu2−O1 bond is 1.897(3) Å indicating that the oxygen of the bridging phenolate is equatorial to Cu2 but apical to Cu1. The Cu1−O1−Cu2 angle is 127.9°, and the phenyl ring of the CH_3HXTA ligand is twisted relative

Table 3. Selected Bond Lengths and Bond Angles for $[Cu_2(CH_3HXTA)(H_2O)_2]H{\cdot}4H_2O$[a]

Bond Lengths (Å)			
Cu1−O1	2.246(4)	Cu2−O6	1.944(3)
Cu2−O1	1.897(3)	Cu2−O8	2.297(4)
Cu1−N1	1.994(4)	Cu1−O10	1.958(4)
Cu2−N2	2.046(4)	Cu2−O11	1.971(4)
Cu1−O4	1.967(3)	Cu1··Cu2	3.726(4)
Bond Angles (deg)			
N1−Cu1−O1	93.7(2)	N2−Cu2−O1	96.1(1)
N1−Cu1−O2	83.3(2)	N2−Cu2−O6	83.4(1)
O1−Cu1−O2	92.1(1)	O1−Cu2−O6	169.2(2)
N1−Cu1−O4	84.8(2)	N2−Cu2−O8	80.5(2)
O1−Cu1−O4	95.5(1)	O1−Cu2−O8	93.4(1)
O2−Cu1−O4	166.3(1)	O6−Cu2−O8	97.2(1)
N1−Cu1−O10	170.9(2)	N2−Cu2−O11	172.4(1)
O1−Cu1−O10	95.3(1)	O1−Cu2−O11	91.4(1)
O2−Cu1−O10	95.0(1)	O6−Cu2−O11	89.2(1)
O4−Cu1−O10	95.7(2)	O8−Cu2−O11	98.9(2)
Cu1−O1−Cu2	127.9(2)		

[a] For labels, see ORTEP drawing.

to the Cu1−O1−Cu2 plane. The resulting dihedral angle between these two planes is 46.7°. This complex is one of only a few with a singly bridging phenoxide ligand providing an open coordination environment.[29−31]

The Cu- -Cu separation in **1** is 3.726 Å. This Cu- -Cu separation is similar to three related singly bridged dicopper(II) complexes.[29−31] $[Cu_2(BBIP)(H_2O)_2]^{+3}$ (where BBIP = 2,6-bis[(bis(benzimidazolylmethyl)amino)methyl]-*p*-cresol) has a Cu- -Cu separation of 3.875 Å, $[Cu_2(BIMP)(CH_3OH)_2]^{3+}$ (where BIMP = 2,6-bis-[(bis(1-methylimidazol-2-yl)methyl)amino)-methyl)-4-methylphenol) has a Cu- -Cu separation of 4.090 Å, and $[Cu_2(BPMP)Cl_2]^+$ (where BPMP = 2,6-bis[[bis(2-pyridylmethyl)amino]methyl]-4-methylphenol) has a Cu- -Cu separation of 4.128 Å. The large Cu- -Cu separations for $[Cu_2(BBIP)(H_2O)_2]^{3+}$, $[Cu_2(BIMP)(CH_3OH)_2]^{3+}$, and $[Cu_2(BPMP)Cl_2]^+$ have been attributed to steric repulsions between the benzimidazole, imidazoyl, and pyridyl groups, respectively, as well as the formation of two adjacent five-membered rings.[29−31] For $[Cu_2(CH_3HXTA)(H_2O)_2]^+$ steric interactions between the terminal carboxylate groups are minimal, so a subtle combination of long Cu-N amine distances compared to the average equatorial Cu-O carboxylate distance (2.020 vs 1.965) and the formation of two adjacent five-membered rings results in the large Cu- -Cu separation. Cu- -Cu separations for doubly bridged complexes utilizing the 2,6-bis(methylamino)-*p*-cresol group are typically in the range 2.9 to 3.3 Å.[23]

The Cu-O aqua bond lengths for **1** are 1.958(4) and 1.971(4) Å, respectively, which are significantly shorter then those observed for related complexes. For comparison, the Cu-O aqua bond lengths for $[Cu_2(BBIP)(H_2O)_2]^{3+}$ and $[Cu_2((Ha)_2(MIPA))(OH)(H_2O)]^{2+}$ (where $(Ha)_2$MIPA = 2,6-bis[((4-imidazoylethyl)-imino)methyl)]-4-methylphenol) are 2.01 are 2.185 Å, respectively.[30,32] The two aqua ligands in $[Cu_2(BBIP)(H_2O)_2]^{3+}$ are trans to an amine nitrogen and a benzimidazole moiety, respectively, while in $[Cu_2((Ha)_2(MIPA))(OH)(H_2O)]^{2+}$ the aqua ligand resides in the apical position. For **1**, both of the aqua ligands are trans to the more weakly bound amine nitrogens.

(29) Nishida, Y.; Shimo, H.; Maehara, H.; Kida, S. *J. Chem. Soc. Dalton Trans.* **1985**, 1945−1951.
(30) Berends, H. P.; Stephan, D. W. *Inorg. Chem.* **1987**, *26*, 749−754.
(31) Oberhausen, K. J.; Richardson, J. F.; Buchanan, R. M.; McCusker, J. K.; Hendrickson, D. N.; Latour, J.-M. *Inorg. Chem.* **1991**, *30*, 1357−1365.
(32) Maekawa, M.; Kitagawa, S.; Munakata, M.; Masuda, H. *Inorg. Chem.* **1989**, *28*, 1904−1909.

Table 4. Electronic Properties of $[Cu_2(X\text{-}HXTA)(L)]$ Complexes

X = OCH_3[a]		X = CH_3[a]		X = Cl[a]		X = CN[a]	
L = $2H_2O$	L = OH^-	L = $2H_2O$	L = OH^-	L = $2H_2O$	L = OH^-	L = $2H_2O$	OH^-
		204 (29.9)		202 (28.8)		204 (23.4)	
238 (6.4)	240 (8.7)	234 (7.5)	240 (9.7)	242 (12.3)	244 (14.9)		214[b] (23.3)
306 (3.1)	308 (3.4)	288 (4.6)	288 (4.4)	292 (5.7)	293 (6.0)	268 (15.1)	270 (18.1)
		340[b] (0.63)	340[b] (0.52)	335[b] (0.71)		320[b] (1.4)	330[b] (1.1)
430 (0.50)	406 (0.45)	420 (0.71)	400 (0.39)	410 (0.47)	390 (0.37)	410 (0.54)	394 (0.42)
750 (0.091)	742 (0.13)	750 (0.13)	750 (0.17)	750 (0.091)	750 (0.14)	746 (0.12)	748 (0.16)

[a] λ_{max}(nm); ϵ(mM^{-1} cm^{-1}) in parentheses. [b] Peaks are shoulders to higher energy transition.

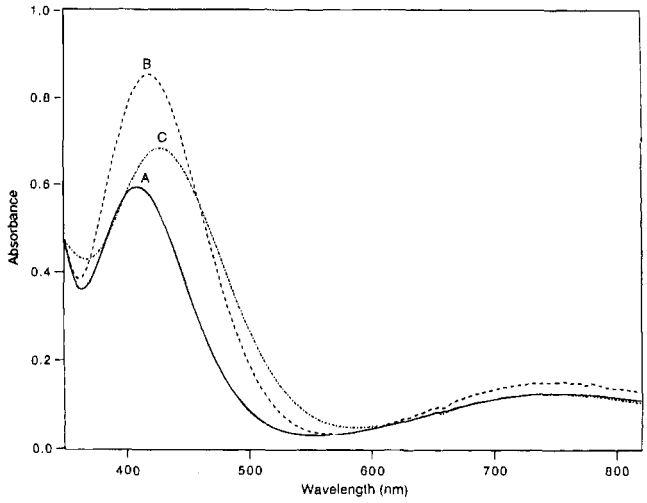

Figure 2. Visible electronic absorption spectra of the $[Cu_2(X\text{-}HXTA)(H_2O)_2]^-$ anion complexes where X = Cl (A), CH_3 (B), and CH_3O (C).

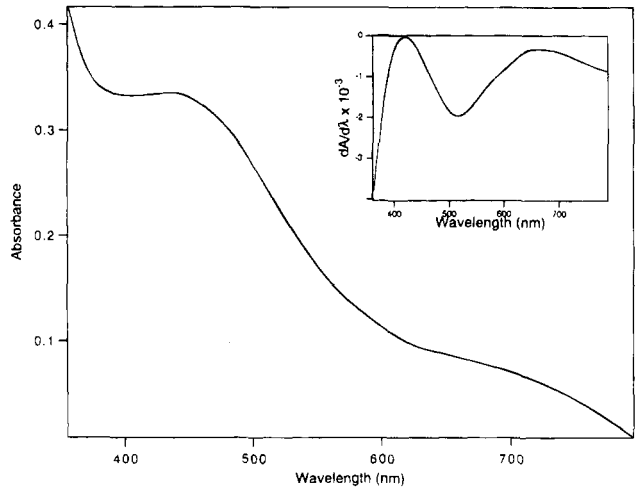

Figure 3. Solid state (Nujol mull) electronic absorption spectrum of **1**. Inset: First derivative spectrum.

This geometrical configuration may contribute to shorter Cu-O aqua bond lengths; however, the more dominant factor is likely the hydrogen bonding interaction between the coordinated water molecule hydrogens and the lattice water molecules. This hydrogen bonding interaction presumably makes the coordinated water molecules more basic which in turn provides shorter Cu-O aqua bond distances.

Electronic Absorption Spectra. Electronic absorption data for the $[Cu_2(X\text{-}HXTA)(H_2O)_2]^{3+}$ anion complexes at pH 3.0 are found in Table 4, and the visible electronic absorption region of these complexes are shown in Figure 2. All of the complexes studied exhibited absorptions in the 200 to 350 nm range that can be attributed to ligand absorption bands and amine- or carboxylate-to-copper ligand-to-metal charge transfer bands (LMCT).[27,30,31,33]

Compound **1** exhibits an absorption band at 420 nm (ϵ = 0.71 mM^{-1} cm^{-1}) that is assigned to a phenoxo-to-copper LMCT band. Similar absorptions are observed for several related (μ-phenoxo)dicopper(II) complexes.[23] Definitive assignment of this band is provided by substitution of the para-methyl group of *p*-cresol with an electron-withdrawing or -donating group. Electron-donating groups are expected to decrease the Lewis acidity of the copper center thus shifting the phenoxo-to-copper charge transfer band to lower energies, while electron-withdrawing groups are expected to increase the Lewis acidity and shift the phenoxo-to-copper charge transfer band to higher energies. When the para-methyl position is substituted with an electron-donating group such as CH_3O, the LMCT band shifts to lower energy (430 nm) (Figure 2). Conversely, when the para-methyl position is substituted with an electron-withdrawing group such as CN or Cl, the LMCT band shifts to higher energy (410 nm) (Figure 2). These energy shifts are consistent with the expected change in the Lewis acidity at the Cu(II) centers thus establishing this band as primarily a phenoxo-to-Cu(II) LMCT band. Similar shifts have been observed for phenoxo-to-iron charge transfer bands in related complexes.[27]

The visible absorption spectrum of **1** also contains a band at 750 nm (ϵ = 0.13 mM^{-1} cm^{-1}) (Figure 2). This band is characteristic of Cu(II) d−d transitions. The position of this band suggests that the geometry about the Cu(II) ions is best described as trigonal bipyramidal.[34] This is in contrast to X-ray data that clearly indicates that each Cu(II) ion resides in a distorted square pyramidal environment. In order to determine the geometry of the Cu(II) ions in solution, a direct comparison of the energies of the ligand field transitions in both the solution and solid states is required. A solid state (Nujol mull) electronic absorption spectrum of **1** was recorded (Figure 3). Two transitions are observed at 420 and 670 nm that correspond to the phenoxo-to-Cu(II) LMCT band and the Cu(II) d−d band, respectively. The position of the d−d band for **1** in the solid state is indicative of a square pyramidal geometry for Cu(II). Thus, the distorted square pyramidal geometry observed for **1** in the solid state is not maintained in solution. This geometrical change may be a result of the relaxation of the strained phenol ring in the solid state and subsequent relaxation if the twisted phenol ring relative to the Cu1−O1−Cu2 plane.

Spectral titration of **1** with sodium hydroxide causes a shift in the LMCT band from 420 to 400 nm with a concomitant decrease in the molar absorptivity (Figure 4; Table 4). These data suggest that **1** can be converted to a second dicopper(II) complex (**2**) by the addition of sodium hydroxide. The conversion of **1** to **2** is completely reversible. A plot of the

(33) Solomon, E. I.; Baldwin, M. J.; Lowery, M. D. *Chem. Rev.* **1992**, *92*, 521−542.

(34) Hathaway, B. J.; Billing, D. E. *Coord. Chem. Rev.* **1970**, *5*, 143−207.

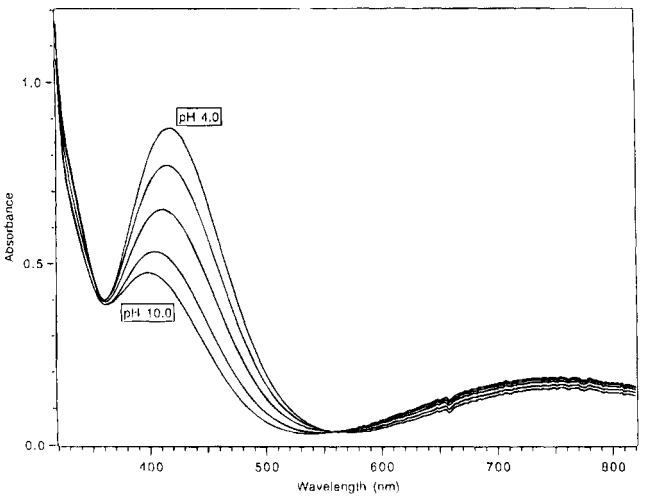

Figure 4. Titration of $[Cu_2(CH_3HXTA)(H_2O)_2]^-$ (1.1×10^{-3} M) with sodium hydroxide (0.1 M) in aqueous solution. Representative spectra correspond $[OH^-]$:$[Cu_2]$ ratios from 0.75 to 1.75.

Scheme 1

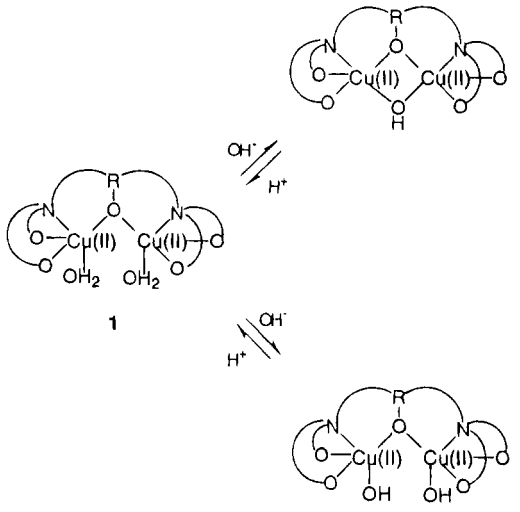

absorbance maximum at 420 to 400 nm vs pH indicates the deprotonation process has an apparent pK_a of 8 to 25 °C. The absorption band at 750 nm for **2** is assigned to a copper d−d band. The position of this band is consistent with a trigonal bipyramidal geometry about the Cu(II) ions.[34]

Two potential reaction pathways for the conversion of **1** to **2** can be envisioned (Scheme 1). The first would involve the deprotonation of one water molecule and the loss of the second resulting in a (μ-phenoxo)(μ-hydroxo)dicopper(II) complex. Alternatively, both coordinated water molecules may be deprotonated giving a (μ-phenoxo)bis(hydroxo)dicopper(II) complex. An isobestic point is observed at 560 nm indicating that intermediates such as an aquahydroxodicopper(II) complex at equilibrium are not detectable. In the absence of X-ray crystallographic data for **2**, differentiation between a (μ-phenoxo)(μ-hydroxo)- or (μ-phenoxo)bis(hydroxo)dicopper(II) complex can be obtained from the magnetic properties of an aqueous solution of **2**.

Magnetic Properties. The X-band EPR spectra of powdered samples of **1** at 298 and 77 K and a frozen aqueous solution of **1** at pH 3.0 at 77 K are shown in Figure 5. The powder spectrum of **1** at 298 K displays an isotropic signal with g = 2.15. Upon cooling this sample to 77 K, the observed signal becomes slightly anisotropic. The observed anisotropy may reflect the distinct Cu(II) centers in **1** or may be due to zero-field splitting. The $\Delta M_s = 2$ transition at $g = \sim 4.5$ expected

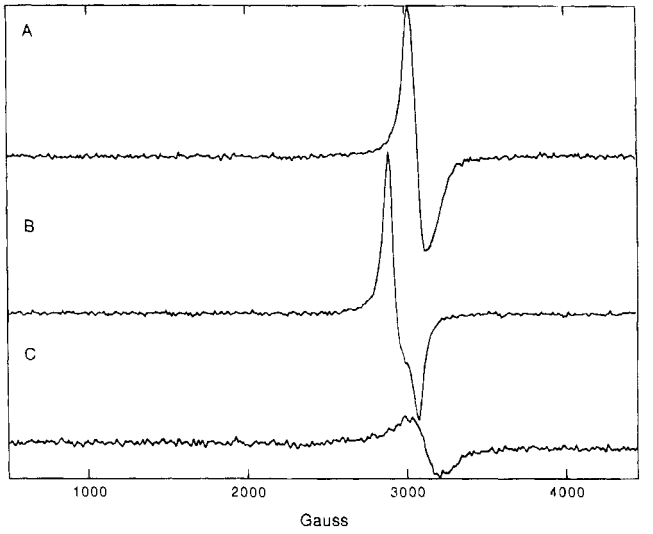

Figure 5. X-band EPR spectra: (A) spectrum for a polycrystalline sample of **1** at 298 K; (B) spectrum for a polycrystalline sample of **1** at 77 K; (C) frozen aqueous solution of complex 1 at 77 K and pH 3.0.

for magnetically coupled Cu(II) ions is not observed for the powder samples, suggesting that the Cu(II) ions in **1** are not magnetically coupled or are very weakly coupled.

Variable temperature magnetic susceptibility data for **1** was collected over the temperature range 10 to 300 K. The shape of the χ_m vs T plot indicates that **1** is a simple Curie−Weiss paramagnet. Simulation of the data using the Curie−Weiss relationship gives $g = 2.16$, $\Theta = -1$, and TIP = 0. The absence of exchange coupling in **1** is due to the fact that the μ-phenoxo oxygen bond is equatorial to Cu2 but apical to Cu1. In dinuclear square pyramidal Cu(II) complexes of this type, the unpaired electron residues in the $d_{x^2-y^2}$ orbital.[29−31] This coordination mode provides no significant orbital overlap between the magnetic orbital $d_{x^2-y^2}$ of Cu2 with the magnetic orbital $d_{x^2-y^2}$ of Cu1, so no exchange coupling occurs. For comparison, the coupling observed for other open type dinuclear Cu(II) complexes with μ-phenoxo bridging ligands such as $[Cu_2(BBIP)(H_2O)_2]^{3+}$, $[Cu_2(BIMP)(H_2O)_2]^{3+}$, and $[Cu_2(BPMP)Cl_2]^+$ are weakly ferromagnetically coupled (+4.2 cm^{-1} and +0.27 cm^{-1}) or uncoupled, respectively.[29−31]

A frozen aqueous solution of **1** at 77 K and pH 3.0 displays an isotropic EPR signal with a g value of 2.13 (Figure 5). The g value obtained from the solution spectrum of **1** at 77 K is consistent with a distorted trigonal bipyramidal geometry about the Cu(II) ions in agreement with the electronic absorption data.[34] EPR spectra recorded on frozen aqueous solutions of **1** at 77 K over the pH range 3 to 10 indicates that the isotropic signal at g = 2.13 disappears with the last detectable signal coming at pH 6. The g value does not change positions as the pH is raised. The loss of a detectable EPR signal for **1** as the pH is increased indicates that the Cu(II) ions are becoming moderately to strongly coupled at high pH values. These data suggest the formation of a (μ-phenoxo)(μ-hydroxo)dicopper-(II) complex at high pH values (Scheme 1).

Since crystalline material of **2** could not be obtained, the Evans susceptibility method,[35,36] was used to determine the magnetic properties of an aqueous solution of **2** at pH 10. The room temperature magnetic moment (μ_{eff}/Cu) of **2** was found to be 1.41 μ_B which gives the number of unpaired electrons

(35) Evans, D. F. *J. Chem. Soc.* **1959**, 2003−2005.
(36) Phillips, W. D.; Poe, M. *Methods Enzymol.* **1972**, *24*, 304−317.

Table 5. ^1H NMR Chemical Shifts at 25 °C for $[Cu_2(HXTA)(L)](X)_n$ Complexes in D_2O

		L = $2H_2O$				L = OH			
signal	assgnt	chem shift[a]	integration[b]	line width[c] (Hz)	T_1[d] (ms)	chem shift[a]	integration[b]	line width[c] (Hz)	T_1[d] (ms)
A	*m*-Ph	14.8	2	240	4	17.8	3	70	7
B	Ph−CH_3	15.7	3	210	11	10.1	2	130	25
C	N−CH_2−CO_2	47[d]	~8[g]	~3100		65	~4	~1400	1
C′	N−CH_2−CO_2					83	~4	~1500	1
D	Ph−CH_2−N	93[f]				143[e]			

[a] All shifts are in ppm relative to the residual solvent signal at 4.7 ppm. [b] Relative areas based on the area of signals A and B.[6] [c] The line widths are full width at half-maximum. [d] T_1 values were obtained at 300 MHz and 30 °C following the methods outlined in ref 6. [e] Signal appears at ~50 °C. [f] Signal appears at ~70 °C. [g] Relative area obtained at 50 °C.

(*n*/Cu) as 0.73. For comparison, the room temperature magnetic moment (μ_{eff}/Cu) of an aqueous solution of **1** at pH 3 was found to be 1.69 μ_B which gives the number of unpaired electrons (*n*/Cu) as 0.97. The decrease in the number of unpaired electrons for **2** compared to **1** suggests that the Cu(II) ions in **2** are moderately antiferromagnetically coupled.

Magnetic data for several other related (μ-phenoxo)(μ-hydroxo)dicopper(II) complexes have been reported.[31,37-39] All of these complexes exhibit moderate to strong antiferromagnetic coupling between the Cu(II) centers with -2J values greater than 100 cm^{-1}. Crystallographic data for similar complexes such as $[Cu_2(BPMP)(OCH_3)]^{2+}$ and $[Cu_2(BIMP)(OCH_3)]^{2+}$ indicate that each Cu(II) ion adopts a trigonal bipyramidal geometry.[31,40] This configuration results in the magnetic orbitals (d_{z^2}) oriented along the methoxide-copper bonds providing moderately antiferromagnetically coupled Cu(II) centers (-2J = 94 cm^{-1} for $[Cu_2(BIMP)(OCH_3)]^{2+}$).[31] Structural correlations for **2** are difficult due to the lack of crystallographic data; however, a trigonal bipyramidal geometry for **2** is consistent with electronic absorption spectra. The lack of an EPR signal for **2** and the magnetic data are consistent with the Cu(II) ions being moderately or strongly coupled, implicating **2** as a (μ-phenoxo)-(μ-hydroxo)dicopper(II) complex.

NMR Spectroscopy. Definitive assignment of **2** as a (μ-phenoxo)(μ-hydroxo)dicopper(II) complex can be deduced from ^1H NMR spectroscopy. ^1H NMR is a natural technique to probe paramagnetic systems since only protons proximate to the paramagnetic center are affected.[41-43] Building on our initial success using NMR spectroscopy to probe dinuclear Cu(II) complexes,[44] we have applied one-dimensional ^1H NMR techniques to both **1** and **2**. Antiferromagnetically coupled Cu(II) centers provide relatively sharp hyperfine shifted ^1H NMR signals since they possess a diamagnetic ($S = 0$) ground state.[45] For **2**, the magnetic moment of the complex is relatively small so isotropically shifted ^1H NMR signals are observed.

Complex **2** shows four isotropically shifted signals in the 100 to 0 ppm chemical shift range at 25 °C in D_2O and pH 10 while **1** shows only two signals (pH 3) (Figure 6, Table 5). All of the isotropically shifted signals for **1** and **2** sharpen and shift toward the diamagnetic region as the temperature is increased. A new broad signal appears for **2** at ~150 ppm at 35 °C but for **1**, one broad signal appears at 47 ppm at 50 °C and another very broad signal appears at 93 ppm at 90 °C. Assignment of the isotropically shifted ^1H NMR signals of **1** and **2** can initially be made by inspection of their peak areas. For **1**, the two observed resonances at 15.7 and 14.8 ppm integrate to 3 and 2 protons, respectively. These signals can be assigned to the meta-phenol and para-methylphenol protons, respectively, since these protons are the furthest from the paramagnetic Cu(II) ions. Replacement of the para-methyl group of **1** with Cl causes the resonance at 15.7 ppm to disappear. These data unequivocally assign this signal (15.7 ppm) to the para-methylphenol protons. For **2**, the resonances at 17.8 and 10.1 ppm integrate to 2 and 3 protons, respectively, and are thus assigned to the meta-phenol and para-methylphenol protons. Likewise, definitive assignment comes by replacing the para-methyl group of **2** with Cl which causes the resonance at 10.1 ppm to disappear.

Assignment of the remaining observed signals for **1** and **2** come from selective deuteration experiments, T_1 values, and

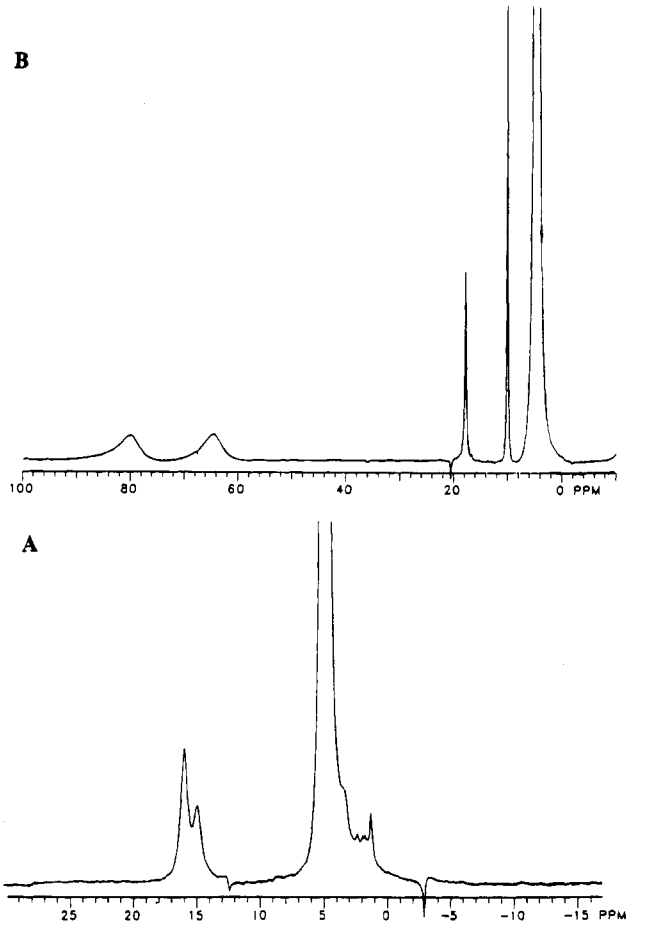

Figure 6. ^1H NMR spectra: (A) spectrum of **1** in D_2O at pH 3.0 and 298 K; (B) spectrum of **2** at pH 10 and 298 K.

(37) Murry, K. S. In *Biological and Inorganic Chemistry of Copper*; Karlin, K. D., Zubieta, J., Eds.; Academic: Guilderland, NY, 1986; Vol. II.
(38) Karlin, K. D.; Farooq, A.; Hayes, J. C.; Brett, I. C.; Rowe, T. M.; Sinn, E.; Zubieta, J. *Inorg. Chem.* **1987**, *26*, 1271−1280.
(39) Sorrell, T. N.; Jameson, D. L.; O'Connor, C. J. *Inorg. Chem.* **1984**, *23*, 190−195.
(40) Maloney, J. J.; Glogowski, M.; Rohrbach, D. F.; Urbach, F. L. *Inorg. Chim. Acta* **1987**, *127*, L33−L35.
(41) Bertini, I.; Luchinat, C. *NMR of Paramagnetic Molecules in Biological Systems*; Benjamin & Cummings: Menlo Park, CA, 1986.
(42) La Mar, G. N.; de Ropp, J. S. *NMR Methodology for Paramagnetic Proteins*; Berliner, L. J., Ed.; Plenum Press: New York, 1993; Vol. 12, pp 1−78.
(43) Bertini, L.; Turano, P.; Vila, A. J. *Chem. Rev.* **1993**, *93*, 2833−2932.
(44) Holz, R. C.; Brink, J. M. *Inorg. Chem.* **1994**, *33*, 4609−4610.
(45) Byers, W.; Williams, R. J. P. *J. Chem. Soc. Dalton Trans.* 1972, 555−560.

relative integrations. For **1**, two additional signals are observed at high temperature whereas one is observed for **2** (Table 5). The two resonances at 83 and 65 ppm for **2** are assigned to the diastereotopic β-CH_2 acetate protons based upon their relative integrations, T_1 values, and the fact that they are selectively deuterated in D_2O solution at 90 °C and pH 10. The β-CH_2 acetate protons should be the most acidic protons of the CH_3-HXTA ligand, and thus deuteration at high pH values and high temperature is not unexpected. The corresponding ^2H NMR experiments show both resonances at the appropriate chemical shifts thus, unambiguously assigning them to the β-CH_2 acetate protons. The only remaining protons in **2** unassigned are the β-CH_2 protons of the phenol−methylamine linkage. These protons can be assigned to the resonance observed at 143 ppm and 55 °C by default and by the fact that these protons are likely closest to the Cu(II) ions and hence will provide the broadest signals. For **1**, the signal at 47 ppm and 50 °C is assigned to the β-CH_2 acetate protons since this resonance disappears when the β-CH_2 acetate protons are deuterated. ^2H NMR experiments shows the corresponding resonance at the appropriate chemical shift value, thus substantiating the assignment to the β-CH_2 acetate protons. By default, the resonance observed at 93 ppm and 90 °C for **1** is assigned to the β-CH_2 protons of the phenol-methylamine linkage.

Comparison of the ^1H NMR chemical shifts of **2** with those of the crystallographically characterized (μ-phenoxo)(μ-hydroxo)dicopper(II) complex $[Cu_2(BPMP)(OH)](ClO_4)_2$,[44] indicate that **2** is a (μ-phenoxo)(μ-hydroxo)dicopper(II) complex. These data, taken together with the spectroscopic and magnetic data for **2**, confirm that at high pH values **1** is converted into the (μ-phenoxo)(μ-hydroxo)dicopper(II) CH_3HXTA complex $[Cu_2(CH_3HXTA)(\mu\text{-}OH)]^{2-}$.

Conclusion and Biological Perspective

We have synthesized and crystallographically characterized a dinuclear Cu(II) complex containing μ-phenoxo bridging ligand with terminal carboxylate oxygen, amine nitrogen, and water ligands. A second complex, generated upon the addition of sodium hydroxide, has been spectroscopically characterized as a (μ-phenoxo)(μ-hydroxo)dicopper(II) complex. These complexes serve as initial models for the active dicopper(II) substituted AP and bILAP enzymes. From recent X-ray crystallographic data on aminopeptidases, the active sites consist of dinuclear Zn(II) or Co(II) centers that contain at least three carboxylate groups and one or two lysine or histidine residues.[9-12] All of the aminopeptidase dinuclear sites are bridged by at least one carboxylate group. The CH_3HXTA ligand, therefore, provides an excellent biomimetic ligand for aminopeptidases since it contains four carboxylate and two amine nitrogen ligating groups. While no spectroscopic or structural data are available for the Cu(II)-substituted AP or bILAP enzymes, the structural and magnetic properties of the complexes reported herein may provide some insight into the structural properties of the active dicopper(II) centers in AP and bILAP. We are currently probing the structural and magnetic properties of the active dicopper(II) AP and bILAP enzymes as well as the hydrolytic activity of the dinuclear Cu(II) CH_3HXTA complexes.

Acknowledgment. This work was supported by the Utah State University Research Office and the Petroleum Research Fund (Grant ACS-PRF 28635-G). The Bruker ARX-400 NMR spectrometer was purchased with funds provided by the National Science Foundation (Grant CHE-9311730) and USU. The authors are also grateful to Professor John L. Hubbard for his assistance in the crystal structure determination. We acknowledge the NSF for partial funding of the X-ray diffractometer (Grant CHE-9002379). C.J.O. wishes to acknowledge support of a grant from the Louisiana Educational Quality Support Fund administered by the Board of Regents of the State of Louisiana for the purchase of the SQUID magnetometer.

Supplementary Material Available: A crystal packing diagram, tables detailing the X-ray data collection and refinement, bond distances, bond angles, final anisotropic thermal parameters, calculated or refined H atom coordinates, and atomic coordinates and equivalent isotropic thermal parameters, a plot of the absorbance maximum at 420 and 400 nm vs pH, and a plot of χ_m vs T for **1** (9 pages). Ordering information is given on any current masthead page.